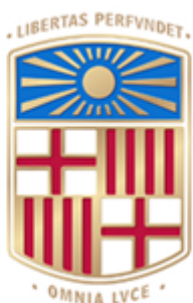


Docking assays of Musashi-1 allosteric RNA-binding sites



Universitat
Oberta
de Catalunya



UNIVERSITAT DE
BARCELONA

Lucas Goiriz Beltrán

MU Bioinf. i Bioest.
Área de trabajo final

Nombre Tutor/a de TF

Emmanuel Fajardo

**Profesor/a responsable
de la asignatura**

Nuria Pérez Álvarez

Fecha Entrega

15 de Enero 2023



Esta obra está sujeta a una licencia de Reconocimiento-NoComercial-SinObraDerivada 3.0 España de Creative Commons

FICHA DEL TRABAJO FINAL

Título del trabajo:	<i>Docking assays of Musashi-1 allosteric RNA-binding sites</i>
Nombre del autor:	<i>Lucas Goiriz Beltrán</i>
Nombre del consultor/a:	<i>Emmanuel Fajardo</i>
Nombre del PRA:	<i>Nuria Pérez Álvarez</i>
Fecha de entrega:	<i>01/2023</i>
Titulación o programa:	<i>Máster Universitario en Bioinformática y Bioestadística</i>
Área del Trabajo Final	<i>Drug Design and Structural Biology</i>
Idioma del trabajo:	<i>Inglés</i>
Palabras clave:	<i>Molecular Docking, RNA-binding protein, Allosteric Regulation</i>
Resumen del Trabajo	
<p>La proteína Musashi-1 (MSI-1) es una proteína de unión a RNA que juega un papel crucial en el desarrollo neuronal tanto en vertebrados como en invertebrados que además también interactúa allostéricamente con ácidos grasos. Estas propiedades hacen que MSI-1 sea una parte biológica interesante en biología sintética para su aplicación como regulador post-transcripcional allostérico de la expresión génética en circuitos généticos sintéticos. Sin embargo, con tal de utilizar con seguridad a MSI-1 como una parte biológica, es necesario entender cómo funcionan sus mecanismos de interacción subyacentes independientemente de los ligandos específicos proporcionados. En este trabajo, se estudian las interacciones allostéricas ocurrientes en MSI-1 mediante simulaciones de docking proteína-RNA y proteína-lípido, a través de una variedad de motivos de RNA sintéticos y de ácidos grasos. Los resultados indican que el comportamiento allostérico de MSI-1 es probablemente debido a un cambio conformacional dentro de la proteína, el cual altera la región de unión a RNA. La eficiencia con la que un ácido graso particular induce este cambio conformacional aún debe ser estudiada, aunque se sugiere que los ácidos grasos más pequeños y flexibles pueden tener una mayor capacidad para inducir cambios conformacionales en la proteína. Los diferentes modelos de interacción proteína-RNA obtenidos fueron inconsistentes para cada motivo RNA, por lo que el efecto de la secuencia nucleotídica del RNA en la interacción continúa sin respuesta.</p>	

Abstract

The Musashi-1 (MSI-1) protein is a neural RNA-binding protein that plays a crucial role in neural development in both vertebrates and invertebrates which also interacts allosterically with fatty acids. These properties make MSI-1 an interesting biological part in synthetic biology for its applicability as an allosteric post-transcriptional regulator of gene expression in synthetic gene circuits. However, in order to confidently use MSI-1 as a biological part, there is a need to understand how its underlying interaction mechanisms work irrespective of the particular ligands provided. In this work, the allosteric interactions occurring in MSI-1 are studied by means of protein-RNA and protein-lipid docking simulations involving a variety of synthetic RNA motifs and several fatty acids. The results indicate that the allosteric behavior of MSI-1 is likely due to a conformational change within the protein that alters the RNA binding region. The efficiency at which a particular fatty acid induces this conformational change is yet to be studied, although it is suggested that smaller and more flexible fatty acid molecules may have a greater ability to induce conformational changes in the protein. The different protein-RNA interaction models obtained were inconsistent within each different RNA motif, so the effect of the RNA nucleic acid sequence itself on the interaction remains unanswered.

Index

1	Introduction	1
1.1	Context and justification	1
1.2	Objectives	3
1.3	Impact on sustainability, social-ethical and diversity	3
1.3.1	Sustainability	3
1.3.2	Social and ethical responsibility	5
1.3.3	Diversity, gender and human rights	5
1.4	Approach and methods	5
1.5	Work plan	6
1.6	Summary of obtained products	8
1.7	Summary of other sections of this report	9
2	State of the art	10
2.1	Synthetic Biology	10
2.2	RNA-binding proteins and the Musashi family	11
3	Materials and methods	13
3.1	Data Acquisition	13
3.1.1	Mouse MSI-1 and MSI-1's RMM1	13
3.1.2	Fatty acids	13
3.2	Generation of 3D RNA molecule structures	14
3.3	Protein-RNA docking simulations with LightDock	15
3.3.1	Protein preparation	16
3.3.2	RNA preparation	16
3.3.3	LightDock setup and simulation	17
3.3.4	LightDock docking simulation, clustering and ranking	17
3.4	Lipid-protein docking simulations with AutoDock Vina	18
3.4.1	Protein preparation	19
3.4.2	Lipid preparation	20
3.4.3	Grid preparation	20
3.4.4	AutoDock Vina simulation	22
3.5	Lipid-protein-RNA complex visualization	22
4	Results	23
4.1	MSI-1's RRM1-orig docking model	23
4.2	MSI-1's RRM1-orig (unstructured) docking model	24
4.3	MSI-1's RRM1-mutant RNA docking models	25
4.4	MSI-1's RRM1-lipid docking models	26
4.5	Lipid-protein-RNA complex visualization	28

5 Conclusions and further work	30
6 Glossary	32
7 References	33
8 Appendix	I
Appendix A: RNA motifs employed in this work, as seen in [1] (in .fasta format)	I
Appendix B: Python script to treat the RNA motifs	I
Appendix C: Python script to relabel HIS residues for their corresponding AMBER94 compatible residues	III
Appendix D: Python to remove 3' and 5' hydroxile groups in the RNA structures	V
Appendix E: Python script to rename and remove incompatible atom types from the RNA srtructure	V
Appendix F: Python script to remove the incompatible R tags from the RNA structures	VIII
Appendix G: Python script to recover the R tags from the RNA structures	VIII
Appendix H: Bash script to cluster and rank the models generated by LightDock	IX
Appendix I: Bash script to run a complete protein-RNA docking simulation with LightDock	IX
Appendix J: Contents of the grid file employed during the protein-lipid docking simulations	XII
Appendix K: Contents of the config file employed during the protein-lipid docking simulations	XII

List of Figures

1	3D RRM1 structure of the MSI-1 protein constructed by means of protein crystallization and RMN.	1
2	3D mouse MSI-1 structure as predicted by AlphaFold.	2
3	Work plan summarized in a Gnatt chart.	8
4	Uniprot entry Q61474 corresponding to the mouse MSI-1.	13
5	3D structure of the fatty acids to be employed.	14
6	RNA sequences along with the result of the pairwise alingments and Nupack's prediction of their secondary structure.	15
7	3D structures of the RNA motifs.	15
8	LightDock setup command.	17
9	LightDock execution command.	18
10	Execution of the <code>run1.sh</code> script.	18
11	Protein models in AutoDock Tools.	19
12	AutoDock Tools generic grid box.	21
13	Execution of a docking simulation with AutoDock Vina.	22
14	Top 10 scoring models for RRM1-orig RNA-motif complex.	23
15	Top 10 scoring models for RRM1-orig RNA-motif complex grouped by RNA conformations.	23
16	Top 10 scoring models for RRM1-orig unstructured RNA-motif complex.	24
17	Top 10 scoring models for RRM1-mutant RNA-motif complexes.	25
18	MSI1's RRM1 colored by aminoacid polarity.	26
19	Top models for RRM1-fatty acid docking simulations.	27
20	Oleic acid-RRM1-original RNA motif complex.	28
21	Top models for RRM1-fatty acid complexes.	29

Acknowledgements

I would like to thank my supervisor Emmanuel Fajardo for guiding me during this work. It was always nice to be reassured, even when I thought that the results obtained weren't good enough or when some objectives had to be discarded and the work schedule had to be restructured.

I would also like to thank Brian Jiménez García, whom I contacted for the possibility to contribute a tutorial for LightDock. It was fantastic talking to him, as he aided me with some tips and hints so that the LightDock docking simulations worked out better. I hope that we get to collaborate again in the future.

Lastly, but no less important, I would like to thank my friends and lab partners María, Raúl and Roser, who were there for me during this difficult period of my life that unfortunately happened to coincide with this Master's Thesis writing. I know things will get better with time, but I doubt I would've made it through this without your unconditional aid. Thank you.

1 Introduction

1.1 Context and justification

The Musashi-1 (MSI-1) protein belongs to a family of neural RNA-binding proteins (RBPs) that play a fundamental role in neural development in both vertebrates and invertebrates [2, 3, 4, 5]. In particular, the mouse MSI-1 consists of 362 aminoacids with a molecular mass of 39 kDa [3], and contains 2 sequences of around 80 to 90 aminoacids that interact with RNA (RRMs; short for RNA-recognition motifs) following the consensus sequence RU_nAGU^{1,2} [5, 7].

Despite multiple efforts, the complete structure of any of the MSI-1 protein homologues remains a mystery. The most notable successes have only been able to completely elucidate MSI-1's RRM1 and RRM2 domains [8, 9, 10, 11], see for example **Figure 1** for the 3D structure of RRM1.

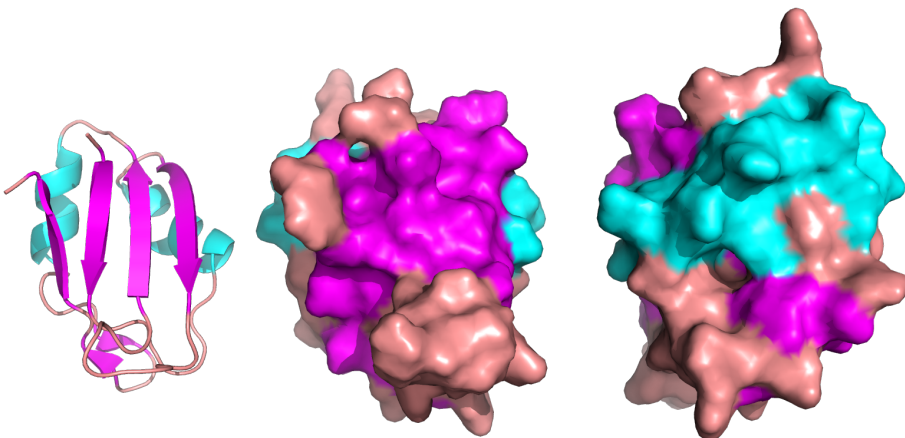


Figure 1: 3D RRM1 structure of the MSI-1 protein constructed by means of protein crystallization and RMN. From left to right: RRM1 in *cartoon* setting, RRM1 in *surface* setting and RRM1 in *surface* setting turned 180°. Colors represent the secondary structures found within the protein: cyan corresponds to α -helices, magenta corresponds to β -sheets and salmon corresponds to *random coil*. The model was retrieved from [Uniprot entry Q61474](#). Visualized through [Pymol](#).

¹Following the IUPAC standard for degenerate base symbols, R represents both an Adenine (A) and a Guanine (G). Refer to [6] for the complete IUPAC standard.

²U_n stands for repeating U within the consensus sequence n times. In most cases, n ∈ {1, 2, 3} [5].

At the moment, the available complete MSI-1 structures only originate from computational predictions, such as the one shown in **Figure 2** which is an aminoacid-sequence-based prediction yielded by [AlphaFold](#) [12].

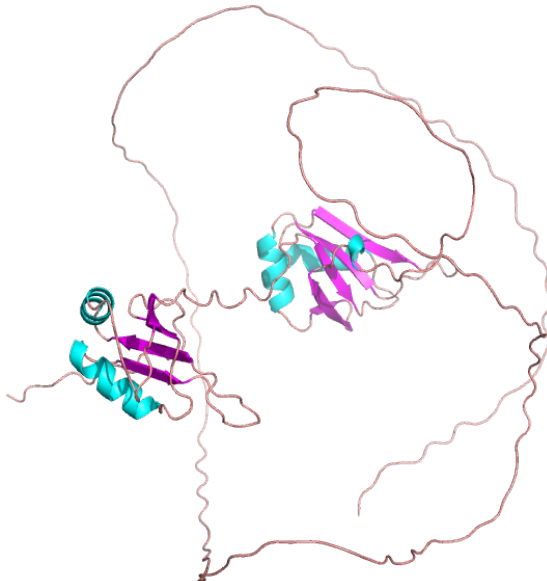


Figure 2: 3D mouse MSI-1 structure as predicted by [AlphaFold](#), in *cartoon* setting. Colors represent the secondary structures found within the protein: cyan corresponds to α -helices, magenta corresponds to β -sheets and salmon corresponds to *random coil*. The model was retrieved from [Uniprot entry Q61474](#). Visualized through [Pymol](#).

With the surge of synthetic biology during the past two decades, RBPs such as MSI-1 have gained a special interest for their applicability as post-transcriptional regulators of gene expression in synthetic gene circuits [13, 14, 15]. In particular, Dolcemascolo and colleagues pioneered by designing a synthetic genetic circuit employing MSI-1 as post-transcriptional regulator [1]. In addition, they also exploited MSI-1's particularity of binding to fatty acids in addition to RNA, out of which the cis-9-Octadecenoic acid (also known as oleic acid) presents a higher binding affinity. The latter interaction weakens the MSI-1 protein's RNA-binding affinity, resulting in a dissociation between MSI-1 and the RNA sequence [1, 16]. In fact, the pocket in which the fatty acids interact with the RMM1 domain of MSI1 can be easily seen in the rightmost protein in **Figure 1**.

Therefore, in order to confidently add MSI-1 as an allosteric regulator to the synthetic biologist's toolbox, there is a need to understand how the underlying interaction mechanisms work. Clingman and colleagues were the first

who performed docking simulations with the MSI-1 core RNA-binding-motif and several fatty acids [16]. Nevertheless, these results only hold for the aforementioned RNA-motif: it is expected that any mutation on the RNA-motif would drastically impact the manner in which MSI-1 interacts with the RNA.

1.2 Objectives

This Master's Thesis aims to extend the knowledge behind the allosteric interactions occurring in the MSI-1 proteins by performing docking simulations between MSI-1's RRM1 domain, several RNA motifs and fatty acids, with the objective of obtaining a model for each of the combinatorial cases.

This general objective breaks down into the following specific objectives:

1. *In silico* Generate the 3D structures of 5 mutant MSI-1 RNA-binding motifs used in [1]. The 3D structures of the motifs will depend on the sequence-based-prediction of their secondary structures.
2. Assess the structure of MSI-1's RRM1-RNA mutant complex through docking for each of the mutants.
3. Assess the structure of MSI-1's RRM1-fatty acid complex through docking for each of the fatty acids of interest: oleic acid, linoleic acid, palmitoleic acid, arachidonic acid and stearic acid.
4. Keep the top 2 fatty acids whose interaction with MSI-1 is the clearest.
5. Assess the structure of RNA mutant-MSI-1's RRM1-fatty acid complex through the coupling of the docking models obtained.

1.3 Impact on sustainability, social-ethical and diversity

1.3.1 Sustainability

The result of this Master's Thesis has had a negligible but negative impact on sustainability. This impact originates on the energy consumption during the following steps:

1. Design and debugging of the docking pipeline followed in this work.
2. Computation of the different models.

This impact can be considered negligible because the net amount of energy consumed during the computations is very small. Nevertheless, it is important to highlight this aspect as there is room for improvement: the source code of the docking software employed in this work is mainly composed of two programming languages: C (72%) and Python (28%).

Pereira and colleagues developed a benchmark to order programming languages with respect of their energy consumption when executing well-known computer science algorithms and data structures [17]. Their finding was that the least energy consuming programming language was C, while Python was one of the most energy consuming.

It can be discussed that, in order to reach minimal energy consumption, the programming language to be used in software that is going to be distributed and executed multiple times should be exclusively C. The disadvantages of C are that it takes more time to write a full program than with higher level languages (such as Python), it is more difficult to maintain a codebase written in C and that C is not a particularly accessible programming language for non-computer scientists.

There is a trade-off that has to be considered. Let L be a programming language, E_{W_L} be the energy consumed by a computer during the crafting of a software written in L , E_{E_L} be the energy consumed by a computer during one execution of the software written in L (in this particular case, one docking simulation with some fixed parameters) and n be the number of times the software is executed, then it is possible to approximate $E_{T_L}(n)$ (the total energy consumed by the software written in L at the moment n) as follows:

$$E_{T_L}(n) \approx E_{W_L} + n \times E_{E_L} \quad (1)$$

For the pair Python and C, we have that $E_{W_{\text{Python}}} << E_{W_C}$ and $E_{E_{\text{Python}}} >> E_{E_C}$. So the larger n becomes (the number of times the software is executed), by **Equation 1**, Python becomes less and less energy efficient when compared to C.

Nevertheless, as mentioned previously, the codebase of the software used is in its majority written in C, the energy consumption of a personal computer is low and the number of executions n in this work is small (less than 10^2). Therefore this negative impact on energy consumption can be considered negligible.

1.3.2 Social and ethical responsibility

The technical nature of this work separates it from any positive nor negative impacts on socio-ethical aspects. There are no conflicts of interests with the results, and this work's material (models and source codes) are freely available to anyone through a public GitHub repository.

In addition, this work doesn't have any socio-ethical motivations, as the main objective is to gather more technical knowledge for the field of molecular biology.

1.3.3 Diversity, gender and human rights

Again, the technical nature of this work separates it from any positive nor negative impacts on diversity, gender and human rights. The references and materials employed within this work were used without any gender nor race bias.

Furthermore, this work doesn't have any diversity, gender nor human rights motivations. However, this work attempts to be accessible to as many people as possible, in the spirit of the universal right for knowledge and education. Moreover, this work exclusively employed license-free and open sourced software so that all the dependencies are accessible to anyone.

1.4 Approach and methods

This work aims to extend the work of Dolcemascolo and colleagues [1] where they designed a synthetic genetic circuit that employed MSI-1 as post-transcriptional regulator. Thanks to the plasticity of RNA, several mutants of MSI-1's RNA-binding core motif were designed, and it was shown that gene regulation (which is tightly dependent on the MSI-1-RNA interaction) was altered for all mutants: some of them displayed an increase in regulation fold change while others displayed a decrease. In addition, the effects of MSI-1 induced regulation were partially nullified in presence of oleic acid.

The initial step of this work will consist in the retrieval of several 3D structures from the appropriate databases:

- the 3D structure of mouse MSI-1's RMM1 is retrieved from [UniProt](#).
- the 3D structures of several fatty acids (oleic acid among them) are retrieved from [chemspider](#).

Next, some of the RNA sequences employed in [1] are retrieved and their 3D model structures are computed by means of [NUPACK](#) and [RNAComposer](#) web server.

Then, all the docking simulations are performed:

1. Between each RNA sequence and MSI-1 RMM1.
2. Between each fatty acid and MSI-1 RMM1.

The choice of docking software will vary for the type of docking simulation to be performed:

- For protein-RNA docking, the docking software will be [LightDock](#) because it is license-free, open source and it is partially written in Python.
- For protein-lipid docking, the docking software will be [AutoDock Vina](#), aided by [AutoDock Tools](#) for the preparation step.

The best models will be selected based on the chosen scoring function and biological significance. In addition, all the models will be visualized with [Pymol](#).

1.5 Work plan

This work is divided in the following tasks (and respective subtasks):

1. Perform docking simulations of MSI-1 and a collection of mutants of the MSI-1 RNA-binding-motif.
 - (a) Generate in silico a collection of up to 5 interesting mutant MSI-1 RNA-binding motifs.
 - (b) Perform docking simulations between MSI-1 and each of the mutants.
 - (c) Discard those mutants whose interaction with MSI-1 is poor.
2. Perform docking simulations of MSI-1 and a collection of fatty acids.
 - (a) Perform docking simulations between MSI-1 and several fatty acids of interest: oleic acid, linoleic acid, palmitoleic acid, arachidonic acid and stearic acid.
 - (b) Keep the top 2 fatty acids whose resulting model is the best.
3. Perform docking simulations of MSI-1 and a subset of mutants of the MSI-1 RNA-binding-motifs in presence of fatty acids.
4. Coupling of the successful docking models to visualize the lipid-MSI1-RNA complex.

5. Defense preparation

- (a) Manuscript
- (b) Presentation

The landmarks of this work are distributed among the following continuous assessment tests:

- Continuous Assessment Test 1: Thesis Definition and Work Plan.
- Continuous Assessment Test 2: Work Development (Phase 1).
Landmarks:
 - Generate in silico a collection of up to 5 interesting mutant MSI-1 RNA-binding motifs.
 - Perform docking simulations between MSI-1 and each of the mutants (*partially*).
- Continuous Assessment Test 3: Work Development (Phase 2).
 - Perform docking simulations between MSI-1 and each of the mutants.
 - Discard those mutants whose interaction with MSI-1 is poor.
 - Perform docking simulations between MSI-1 and several fatty acids of interest: oleic acid, linoleic acid, palmitoleic acid, arachidonic acid and stearic acid (*partially*).
- Continuous Assessment Test 4: Thesis Closure and Presentation.
 - Perform docking simulations between MSI-1 and several fatty acids of interest: oleic acid, linoleic acid, palmitoleic acid, arachidonic acid and stearic acid.
 - Keep the top 2 fatty acids whose resulting model is the best.
 - Manuscript closure.
 - Presentation closure.

The work plan is summarized in **Figure 3**:

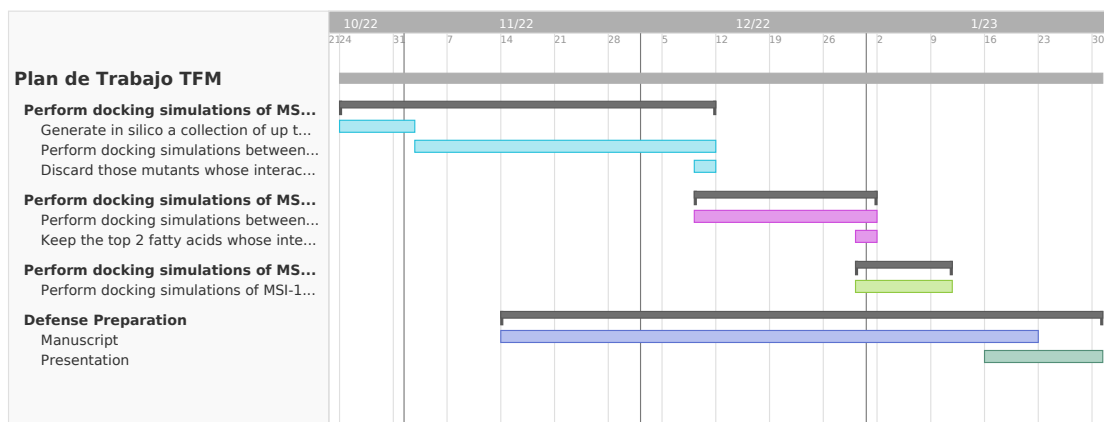


Figure 3: Work plan summarized in a Gnatt chart.

1.6 Summary of obtained products

The main products of this work are:

1. The current Master's Thesis manuscript.
2. 3D structures of 5 MSI-1 RNA-motifs used in [1].
3. A series of Python and Bash scripts used to execute the docking pipeline.
4. A total of 50 protein-RNA docking models (10 for each RNA-motif).
5. A total of 45 protein-lipid docking models (9 for each fatty acid).
6. [A step-by-step tutorial on how to perform a simple protein-RNA docking with LightDock.](#)

Resulting products are available in different repositories:

1. The direct products of this work are present in [this GitHub repository](#).
2. The step-by-step tutorial on how to perform a simple protein-RNA docking with LightDock is available at [the LightDock GitHub repository](#), and on the [LightDock tutorials page](#).

1.7 Summary of other sections of this report

The remaining sections of this manuscript are:

- **State of the art**

Introduction to Synthetic biology, RNA-binding proteins and the Musashi-1 RNA-binding protein family.

- **Materials and methods**

Detailed description of the procedure followed within this work

- **Results**

Main findings, their biological meanings and showcasing of the obtained products.

- **Conclusions and further work**

The findings obtained are discussed in context of this work's original objectives. Further work that can extend this Master's Thesis is described.

- **Glossary**

- **References**

- **Appendix**

2 State of the art

2.1 Synthetic Biology

Synthetic Biology is a modern niche of Biology in which the characteristic “know-how” from engineering fields is combined with classical Molecular Biology techniques. Guided by physicist Richard Feynman’s famous quote “*what I cannot create, I do not understand*”, synthetic biologists have developed a deep understanding of how cells control and regulate the processes of gene transcription, translation, metabolite biosynthesis and degradation.

It is “synthetic” in the sense that synthetic biologists engineer novel (absent in nature) genetic constructions with biological “pieces”, which usually originate from various different organisms, in order to achieve a phenotype in a target organism that lacks said phenotype in nature. Furthermore, this design usually comes with a mathematical model based in physical first principles of how the system should behave.

One of the first successful constructions of this type, and most likely the most popular one, is Gardner’s toggle switch [18] where they engineered a synthetic toggle switch within *E. coli* by using two different promoters that repressed each other, achieving this way bistability (either one promoter is repressed, or the other). Simultaneously, Elowitz’ repressilator [19] was published, where they engineered a synthetic “clock” within *E. coli* by chaining 3 repressive promoters that repressed one another in chain, in such a way that the genes controlled by them had periodic expression.

These constructions, and all the ones that followed, would not have been possible without a (by then, small) repository of genetic parts, which in turn would not have been possible without the arduous work of an innumerable amount of traditional molecular biologists that sequenced and characterized said parts. In fact, the iGEM foundation keeps a repository of standarized biological parts [20] along with various data such as the assembly methods used, levels of expression, polymerase used, etc...

However, there is still a need for more biological parts, especially parts that are “orthogonal”, i.e. they can co-exist and function correctly within the same organism without deviating from their theoretical behavior. This need, plus the known plasticity of the RNA macromolecule, have led to a growing interest in synthetic constructions where gene expression is either directly controlled by RNA [21, 22] or by an RNA-binding protein [13, 14, 15, 23].

2.2 RNA-binding proteins and the Musashi family

RNA-binding proteins (RBPs) are a huge family of proteins that can be found among all domains of life (Bacteria, Archaea and Eukaryota) [24, 25, 26] and can be traced back to the common ancestor of life LUCA [27]. It is therefore no surprise that RBP are still the cornerstone of the majority of cellular processes [26] as they govern mRNA metabolism: mRNA localization, mRNA translation, mRNA degradation, mRNA editing and mRNA stability [28].

The mechanisms in which RBPs interact with RNA differ vastly from DNA-binding proteins (which usually target the double stranded DNA major groove) because RNA comes in a vast variety of structures [28, 29]. The latter can be observed in the shape or sequence specificity displayed by the great variety of known RNA-binding domains (RBDs) [30].

For instance, a popular RBD is the RNA-Recognition Motif (RRM). RRMs typically have a length between 90 and 100 aminoacids (although this can vary), display a $\beta\alpha\beta\beta\alpha\beta$ topology (where β stands for the β -sheet secondary structure and α stands for the α -helix secondary structure), they target single-stranded RNA and are usually present in multiple copies within the same protein, because their interaction with RNA by themselves is weak [28].

The latter makes RBPs containing RMMs interesting candidates for biological parts in synthetic biology, as they display two levels of “tuneability”: the number of RMMs present within the protein and the inherent plasticity of the RNA sequence recognized by them. Such characteristics are present in the homologues of the Musashi (MSI) family of RBPs. For instance, the mouse MSI-1 which consists of 362 aminoacids with a molecular mass of 39 kDa [3] contains 2 RMMs (dubbed RMM1 and RMM2) that interact with RNA containing the consensus sequence RU_nAGU [5, 7].

MSI-1 has an additional particularity that distinguishes it from the common bunch of RBPs, and that is the capability of binding to fatty acids and weakening the MSI-1 protein’s RNA-binding affinity, resulting in a dissociation between MSI-1 and the RNA sequence [1, 16]. This property plus the inherent properties of RMM-based RBPs make MSI-1 a valuable biological part for synthetic biology as a highly tuneable allosteric regulator, as shown by Dolcemascolo and colleagues [1]. However, this presumed tuneability is not yet deeply understood.

Clingman and colleagues made great discoveries of MSI-1's interaction mechanisms [16] by means of docking assays between different fatty acids and the MSI-1-RNA complex. Nevertheless, due to the plasticity of RNA, the obtained results aren't extrapolable to other RNA motifs that MSI-1 may recognize.

For that reason, this work attempts to shed light on the allosteric interactions occurring in the MSI-1 proteins by performing docking simulations between MSI-1's RRM1 domain, several RNA motifs and fatty acids.

3 Materials and methods

3.1 Data Acquisition

3.1.1 Mouse MSI-1 and MSI-1's RMM1

[Uniprot's database](#) was consulted for the structure of the mouse MSI-1 protein (see **Figure 4**). Unfortunately, there was no NMR crystal structure for the complete protein: the only available complete structure was AlphaFold's prediction of the structure (see **Figure 2**). Said structure had low confidence in the aminoacid sequence not corresponding to the RRM1s. Therefore, the crystal structure of MSI-1's RRM1 (see **Figure 1**) was to be employed instead for the docking simulations.

Q61474 · MSI1H_MOUSE

Protein ⁱ	RNA-binding protein Musashi homolog 1	Amino acids	362
Gene ⁱ	Msi1	Protein existence ⁱ	Evidence at protein level
Status ⁱ	UniProtKB reviewed (Swiss-Prot)	Annotation score ⁱ	5/5
Organism ⁱ	Mus musculus (Mouse)		

Entry Feature viewer Publications External links History

BLAST Align Download Add Add a publication Entry feedback

Functionⁱ

RNA binding protein that regulates the expression of target mRNAs at the translation level. Regulates expression of the NOTCH1 antagonist NUMB. Binds RNA containing the sequence 5'-GUUAGUUAGUUAGUU-3' and other sequences containing the pattern 5'-(GA)U(1-3)AGU-3'. May play a role in the proliferation and maintenance of stem cells in the central nervous system. [2 Publications](#)

Figure 4: [Uniprot entry Q61474](#) corresponding to the mouse MSI-1 (as seen on 08/01/2023).

The crystal NMR structure was downloaded as a .pdb file.

3.1.2 Fatty acids

The fatty acids to be employed down the line in the docking simulations were retrieved from their respective [Chemspider](#) entries. The fatty acids downloaded were:

- arachidonic acid
- linoleic acid
- oleic acid

- palmitic acid
- stearic acid

The molecules are shown in **Figure 5**.

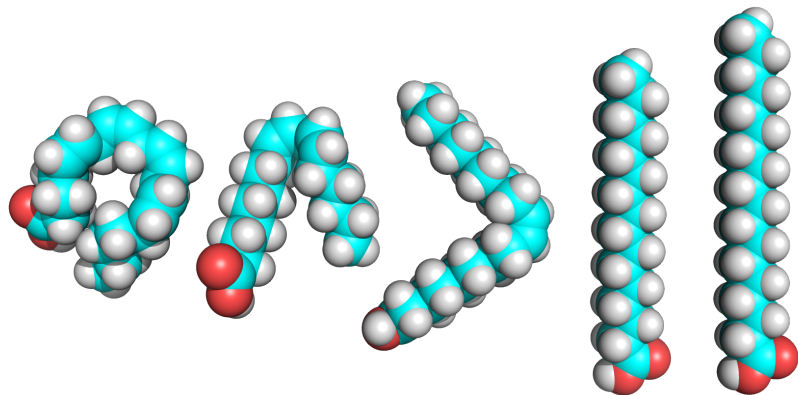


Figure 5: 3D structure of the fatty acids to be employed. From left to right: arachidonic acid, linoleic acid, oleic acid, palmitic acid and stearic acid. Colors represent the atoms present in the structures: cyan is Carbon, red is Oxygen and white is Hydrogen. Visualized through [Pymol](#).

The molecules' 3D structures were downloaded as .mol files.

3.2 Generation of 3D RNA molecule structures

The raw RNA sequences to be employed were retrieved from [1] and are shown in **Appendix A: RNA motifs employed in this work, as seen in [1] (in .fasta format)**, where they crafted small RNA oligos based on the selex optimal RNA sequence. RNA takes specific spatial conformations when in aqueous media, be it *in vitro* or *in vivo*, which can be computed directly from the RNA sequence by means of pre-measured experimental parameters [31].

To do so, the Nupack software was employed [32] (specifically its associated Python package) and the structures in dot-bracket notation³ were recorded. In addition, the sequences were subjected to pairwise alignments (by means of MAFFT [34]) to highlight the mutations present with respect to the original oligo. The Python script employed to perform these computations is found in **Appendix B: Python script to treat the RNA motifs**.

³Dot-bracket notation is a simplistic manner of representing DNA or RNA secondary structure. For more details, see [33].

The results are shown in **Figure 6**:

```
1 name seq alignment structure
2 0 orig GGCAGCGGUUAAGGUUAUAGGUUCGCC ****..... ((((((((. ....) ..))))..)))
3 1 mut1 GGCAGCGGUUCGUUAUAGGUUCGCC ..... * (((((((. ....) ..))))..)))
4 2 mut2 GGCAGCGGUACGUUAUAGGUUCGCC ..... * (((((((....)))..))))..))
5 3 mut3 GGCAGCGGUAGGUUAUAGGUUCGCC ..... * ((((((((....))))..))))..))
6 4 mut4 GGCAGCGGUAGGUAGGUUCGCC ..... * (((((((. ....) ..))))..)))
7 5 mut5 GGCAGCGGUACGUUAUAGGUUCGCC ..... * (((((((....))))..))))..))
```

Figure 6: RNA sequences along with the result of the pairwise alignments and Nupack's prediction of their secondary structure.

With this information (RNA sequence and secondary structure), the 3D conformation of each of the RNA motifs was computed by means of the [RNAComposer](#) web server [35] and downloaded in .pdb format. The corresponding 3D structures of the RNA motifs are shown in **Figure 7**.

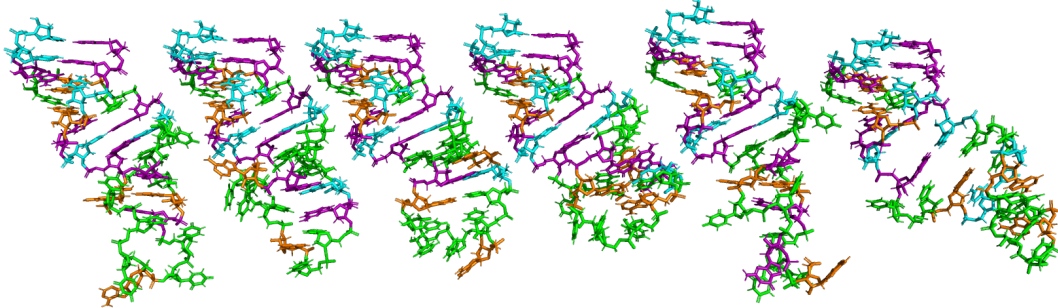


Figure 7: 3D structures of the RNA motifs. From left to right: the original RNA motif followed by the 5 mutants. Colors represent the nucleotidic bases: orange is Adenine, purple is Guanine, cyan is Cytosine and green is Uracil. Visualized through [Pymol](#).

With the 3D structures of the RNA motifs, the next step is to prepare the protein-RNA docking simulations.

3.3 Protein-RNA docking simulations with LightDock

For the protein-RNA docking simulations, the LightDock [36] docking software was chosen. The main reasons are the simplicity of LightDock, the quality of the documentation and that the software is written in Python, which eases debugging steps in case of complications. Originally, LightDock was not meant

for protein-RNA docking simulations. However, by means of some research and auxiliary Python scripts, a simple and novel pipeline was designed which makes it possible to perform such docking simulations with LightDock. This pipeline takes inspiration on the [protein-DNA docking example tutorial from the LightDock documentation](#).

3.3.1 Protein preparation

First, MSI-1's RRM1 .pdb file needs to have their hydrogen atoms modified and relabeled so that they match the AMBER94 force field, which is the parameter set that is going to be used in this docking simulation. To do so, the softwares [REDUCE](#) and [PDB-Tools](#) [37] were employed.

In addition, the MSI-1's RRM1 .pdb file needed an additional modification related to the AMBER94 force field: regular .pdb files employ the HIS identifier for the histidine aminoacid, which does not appear in the AMBER94 force field. The reason behind this is that for the AMBER94 force field, histidine can be one of 3 possible residues [38]:

1. HID: histidine with a single hydrogen on the delta nitrogen
2. HIE: histidine with a single hydrogen on the epsilon nitrogen
3. HIP: histidine with hydrogens on both nitrogens (delta and epsilon). This histidine has a positive charge

Therefore, one has to check which kind of histidine residue is present in the molecule, and change it for the corresponding AMBER94-compatible identifier. This can be done with a simple Python script called `fixHIS`, which is found in **Appendix C: Python script to relabel HIS residues for their corresponding AMBER94 compatible residues**.

3.3.2 RNA preparation

Similar to the protein, the RNA structures' .pdb file need to have their hydrogen atoms modified and relabeled. Again, the softwares [REDUCE](#) and [PDB-Tools](#) [37] were employed.

In addition, REDUCE adds the 3' and 5' hydroxile groups to the RNA structures. These atoms aren't present in the AMBER94 force field, therefore it is mandatory to remove them in order to avoid issues downstream. This can be done with a simple Python script called `removeEnds.py`, which is found in **Appendix D:**

Python script to remove 3' and 5' hydroxile groups in the RNA structures.

Next, due to particularities of REDUCE for nucleic acids, it is necessary to rename and remove incompatible atom types present in the RNA structure. Again, this can be done with a simple Python script called `reduce_to_amber.py`, which is found in **Appendix E: Python script to rename and remove incompatible atom types from the RNA srtructure**. Note that the aforementioned Python script is an adaptation of the original version provided in the [protein-DNA docking example tutorial from the LightDock documentation](#).

Finally, in order to sucessfully run LightDock's setup phase, it is mandatory to remove the R tags within the RNA structures. The R tags are important because they indicate which AMBER94 parameters to use during the docking simulations, however one of LightDock's dependencies in the setup phase ([ProDy](#)) has conflicts with this notation. This removal can be done with a simple Python script called `manipulateRNA.py`, which is found in **Appendix F: Python script to remove the incompatible R tags from the RNA structures**.

3.3.3 LightDock setup and simulation

LightDock's setup itself is simple, as it only consists of executing the setup script with the structures prepared in the previous steps, as shown in **Figure 8**:

```
1 lightdock3setup.py protein.pdb rna.pdb -anm
```

Figure 8: LightDock setup command.

The setup will generate, among other files, the simulation-ready structures `lightdock_protein.pdb` and `lightdock_rna.pdb`. For the docking simulation to be successful, it is crucial to add the R tags within the `lightdock_rna.pdb` RNA structure, which is basically reversing the tag removal process performed earlier. This can be achieved with a simple Python script called `manipulateRNAagain.py`, which is found in **Appendix G: Python script to recover the R tags from the RNA structures**.

3.3.4 LightDock docking simulation, clustering and ranking

If the previous steps executed without issues, it is possible to run LightDock as shown in **Figure 9**:

```
1 lightdock3.py setup.json 100 -s dna -c 4
```

Figure 9: LightDock execution command, using the DNA scoring function for nucleic acids and 4 processing cores.

Once the simulation ends, and in order to be able to do the clustering and ranking step, it is mandatory to remove the R tags added to `lightdock_rna.pdb` for the simulation step. For that, once again the script `manipulateRNA.py` shown in **Appendix F: Python script to remove the incompatible R tags from the RNA structures** is employed.

Next, the clustering and ranking can be performed in the same way as specified in the [protein-DNA docking example tutorial from the LightDock documentation](#). The bash script performing the ranking and clustering steps is shown in **Appendix H: Bash script to cluster and rank the models generated by LightDock**.

The ranking will generate a `solutions.list` file where the different models generated by LightDock are scored. For this work, the top 10 best scoring models were taken.

The entire pipeline followed in this section has been implemented as a bash script called `run1.sh`, which is found in **Appendix I: Bash script to run a complete protein-RNA docking simulation with LightDock**. Given a `target_protein.pdb` file and a `ligand_rna.pdb` file, `run1.sh` is executed as shown in **Figure 10**:

```
1 bash run1.sh target_protein.pdb ligand_rna.pdb
```

Figure 10: Execution of the `run1.sh` script.

A refined version of this pipeline has been contributed to the [official LightDock tutorials section](#). In said version, the Python scripts for file manipulation have been cleaned-up and applied to model the [1A1T protein-RNA complex](#). This tutorial can be directly accessed [here](#).

3.4 Lipid-protein docking simulations with AutoDock Vina

For the lipid-protein docking simulations, AutoDock Vina docking software was employed. The main reasons for changing the docking software at this step

are that for now LightDock does not feature full support of lipid-protein docking and that AutoDock Vina is license free. For the preparation steps, the AutoDock Tools is used for simplicity, although other software could have been used instead.

3.4.1 Protein preparation

First, MSI-1's RRM1 .pdb is loaded into AutoDock Tools, which displays all the models present in said file, as show in **Figure 11**:

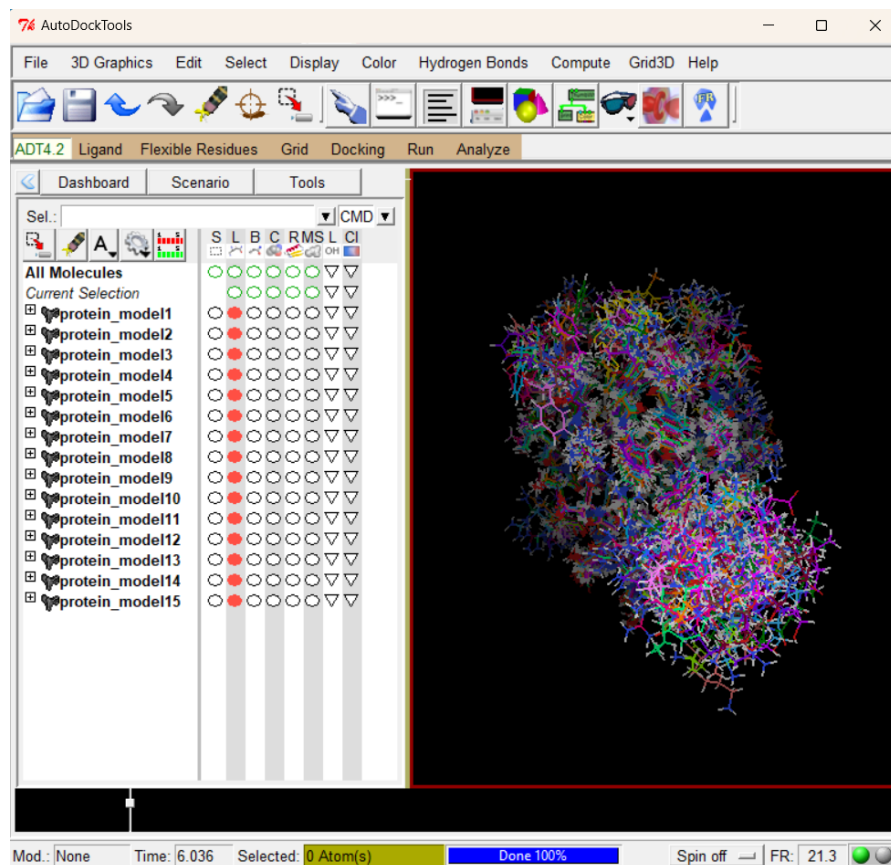


Figure 11: Protein models in AutoDock Tools.

It is mandatory to discard the models that are not going to be used in the docking simulations. For simplicity, in this work the model to be kept is the first one.

Next, there are a series of procedures to prepare the protein model for docking:

1. Remove the water molecules by clicking Edit>Delete Water. This step may be skipped if there are no water molecules present.

2. Add polar hydrogen atoms by clicking Edit>Hydrogens>Add and then select Polar Only. Again, this step may be skipped if the hydrogen atoms are already present.
3. Add Kollmann charges by clicking Edit>Charges>Add Kollmann Charges. This step is unskippable and it is essential for the docking simulation to be successful.

Once these steps are completed, the protein model is ready for docking and can be saved in .pdbqt format by clicking Grid>Macromolecule>Choose....

3.4.2 Lipid preparation

The fatty acid molecules also need a preparation step prior to the docking simulation. First, it is necessary to convert the fatty acid models from .mol format to .pdb format. One way to do this is to open the .mol file in [Pymol](#) and then saving it in .pdb format. An alternative way would be to use an online file converter, such as [this one](#).

Next, the fatty acid in .pdb format is loaded into AutoDock Tools, where preparation is done by clicking Ligand>Input>Choose... and selecting the fatty acid by clicking Select Molecule for AutoDock4. This will remove hydrogens and compute charges, which renders the fatty acid ready for docking. The model is then exported by clicking Ligand>Output>Save.

3.4.3 Grid preparation

One requirement for running AutoDock Vina is knowing the “pocket” which the ligand molecule interacts with. This site is specified by a hexahedron that delimits the spatial area where this site resides (i.e. a grid box), as shown in **Figure 12**.

If the binding “pocket” is unknown, the grid box can be made big so that several conformations around the protein are explored. In the case of MSI-1’s RRM1, the binding pocket that interacts with the fatty acids was described in detail by Clingman and colleagues [16], and can be seen easily in the rightmost protein of **Figure 1**.

With this information, the grid box was manually restrained and exported by clicking File>Output grid dimensions file. The grid dimensions file can be

found in **Appendix J: Contents of the grid file employed during the protein-lipid docking simulations**. The selected grid box will be remain the same for all the protein-lipid docking simulations, because the target protein (MSI-1's RRM1) will remain unchanged.

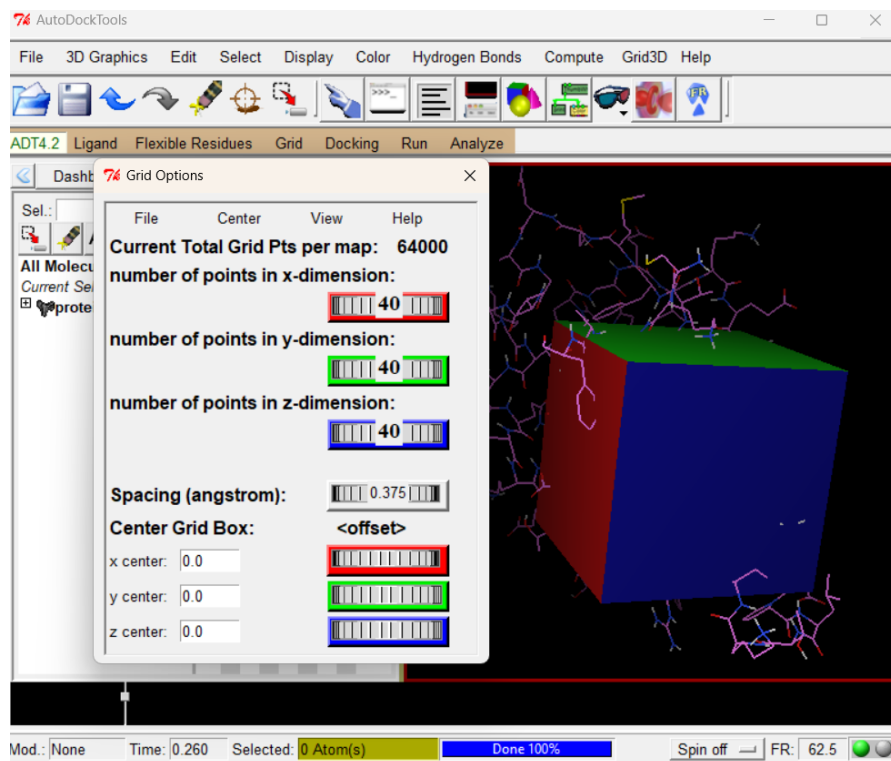


Figure 12: AutoDock Tools generic grid box.

Next, the config file for AutoDock Vina has to be created. This file must contain the protein model name, the ligand model name, the information found in the grid file and two additional parameters: energy range and exhaustiveness. For the latter two parameters, which control the energy spread between the best and the worst output models and the number of times the simulation is executed respectively, the default parameters range = 4 and exhaustiveness = 8 are employed. The config file to be used in the protein-lipid docking simulations can be found in **Appendix K: Contents of the config file employed during the protein-lipid docking simulations**.

The following step is to run the docking simulation itself.

3.4.4 AutoDock Vina simulation

Running a docking simulation with AutoDock Vina requires the prepared protein model in .pdbqt format, the prepared ligand model in .pdbqt format and an appropriate config file. Then, a simulation is run with the command shown in **Figure 13**:

```
1 vina --receptor protein.pdbqt --ligand ligand.pdbqt --config
  config --log log --out output.pdbqt
```

Figure 13: Execution of a docking simulation with AutoDock Vina.

The file `output.pdb` contains the result of the docking simulation and consists of the ligand molecule in 9 different conformations. The `log` file contains information related to the run and the energy scores of each of the conformations. The visualization of the docking simulation result is done by loading the protein model and the `output.pdb` file simultaneously in a software such as [PyMol](#).

3.5 Lipid-protein-RNA complex visualization

The visualization of the lipid-protein-RNA is done by manually aligning the models of the protein-RNA docking simulations with the models of the protein-lipid docking simulations. This procedure is not conceptually optimal, as the correct approach would be to perform a 2 molecule to 1 protein docking simulation, or a docking simulation where the receptor protein is already in contact with the RNA but not with the fatty acid.

However, the latter procedures are not possible due to the atom incompatibilities of the docking models given by LightDock and AutoDock Vina: for the models to be compatible for an AutoDock Vina simulation, it would be necessary to perform a soft molecular dynamics simulation on the LightDock model to fix nicked bonds within the molecular structures, which is out of scope of this work.

As an alternative, a simultaneous visualization can yield insights on the underlying mechanisms of the allosteric interactions in MSI1's RRM1. This visualization is done by means of [PyMol](#).

4 Results

4.1 MSI-1's RRM1-orig docking model

The first docking simulation performed with LightDock corresponded to the RRM1-orig RNA-motif complex. The simulation yielded several models out of which 10 were visualized, as shown in **Figure 14**:

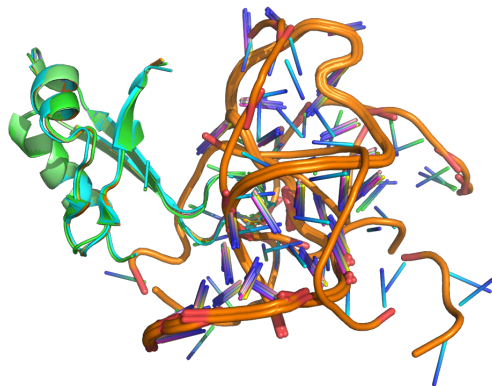


Figure 14: Top 10 scoring models for RRM1-orig RNA-motif complex. Visualized through [Pymol](#).

It is observed that there is no consensus among the top 10 scoring models, as it seems that the RNA-motifs adopts different conformations. To be more precise, in **Figure 14** there are 3 different RNA conformations. Their separate conformations are shown in **Figure 15**:

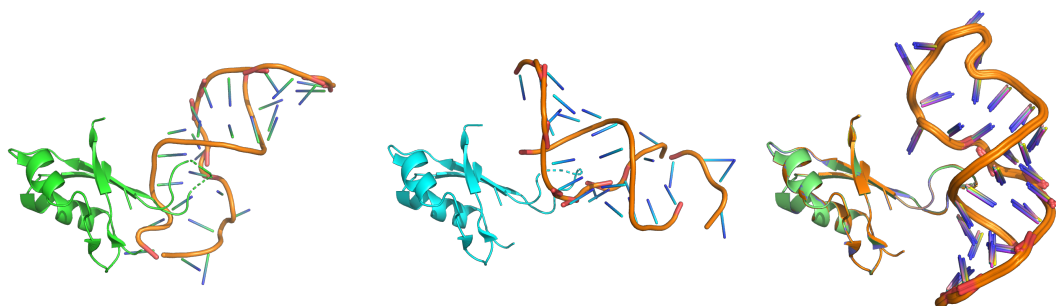


Figure 15: Top 10 scoring models for RRM1-orig RNA-motif complex grouped by RNA conformations. From left to right: best scoring model, second best scoring model and top 3 to 10 best scoring models. Visualized through [Pymol](#).

These models have all in common that MSI1's RRM1 interacts with the RNA motif through the DPLTKRS⁴ loop by inserting itself into a groove present in the secondary structure of the RNA. Clingman and colleagues [16] observed a similar interaction with their unstructured RNA. The interactions presented in **Figure 15** have maintained the RNA self-folding almost intact, which may not occur in reality, as proteins have natural capabilities of disrupting nucleic acid base pairing hydrogen bonds (see for example the Helicase).

Thus, it is natural to reason that the interaction occurring in nature must be an intermediate structure between Clingman's unstructured RNA and the structured RNA shown in **Figure 15**.

4.2 MSI-1's RRM1-orig (unstructured) docking model

To account for the scenario in which the RNA is unstructured (i.e. lacking the natural secondary structure), another docking simulation was executed, which yielded the models shown in **Figure 16**:

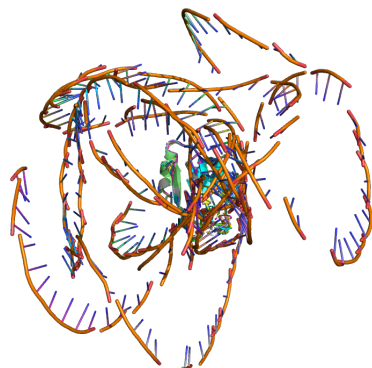


Figure 16: Top 10 scoring models for RRM1-orig unstructured RNA-motif complex. Visualized through [Pymol](#).

There is no consensus among structures. In fact, it seems that long stretches of unstructured RNA do not perform well in docking experiments, as due to the aggressiveness of the docking models, the RNA strand breaks down in multiple regions (more than their structured counterparts) and interactions seem spuri-

⁴Aspartic acid - Proline - Leucine - Threonine - Lysine - Arginine - Serine loop present in RRM1

ous all around the protein surface.

4.3 MSI-1's RRM1-mutant RNA docking models

The simulation with each of the mutants yielded the models shown in **Figure 17**:

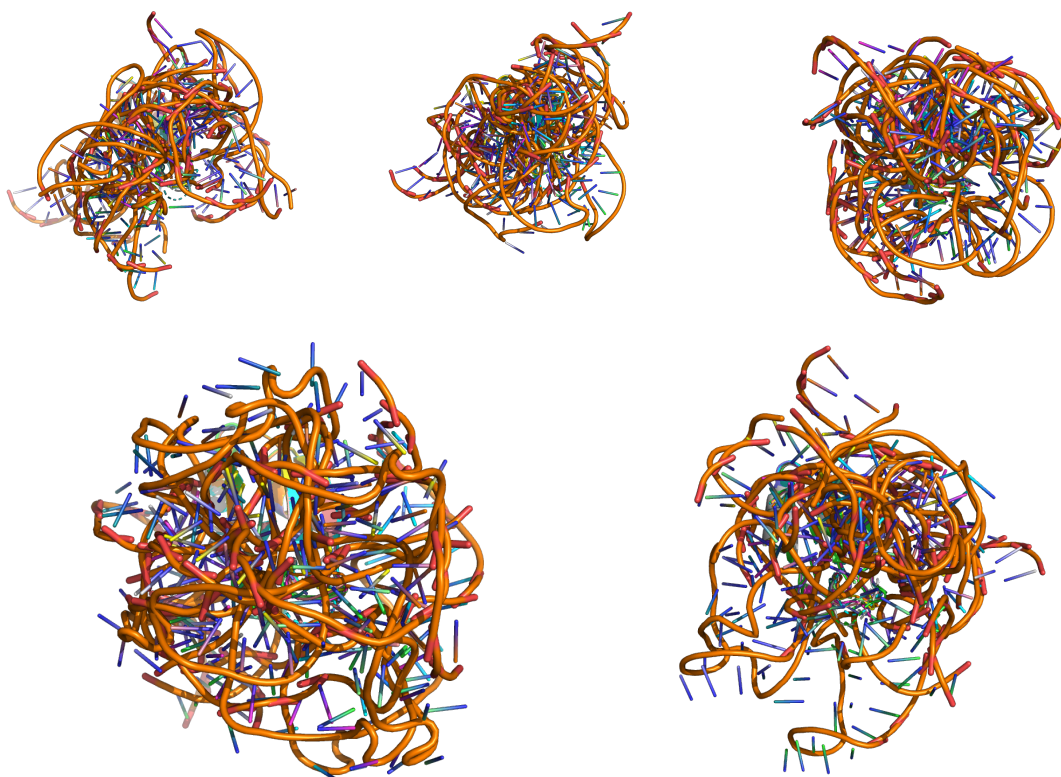


Figure 17: Top 10 scoring models for RRM1-mutant RNA-motif complexes. From left to right and top to bottom: models for RRM1-mutant 1, RRM1-mutant 2, RRM1-mutant 3, RRM1-mutant 3 and RRM1-mutant 5. Visualized through [Pymol](#).

The resulting models do not reach consensus for any mutant and are unsatisfactory. This phenomenon contrasts with the models obtained for the original RNA motif, which are quite similar among them. Dolcemascolo and colleagues [1] designed these mutants in such a way that interaction between MSI-1 and the RNA was just slightly altered, observing in general a slight loss of affinity. An interaction similar to that of the original RNA motif was expected, which was

also backed by the similarity of secondary structures among the original RNA motif and the mutants (especially for mutants 1, 2 and 3. See **Figure 7**).

It is surprising to observe that the supposed interaction is altered in such a drastic way by only point mutations. Thus, either MSI-1 is extremely sensitive with respect to the interacting RNA sequence or *ab initio* docking is not sufficient to obtain good protein-RNA docking models.

4.4 MSI-1's RRM1-lipid docking models

The protein-lipid docking experiments were carried out with AutoDock Vina, and contrary to the previous docking simulations shown within this work, were not *ab initio* as the spatial region where the fatty acid is supposed to interact was given as a constraint. Given the polarity of MSI1's RRM1's surface (see **Figure 18**), especially within the fatty acid-binding pocket, it is expected for the fatty acid to expose their carboxylic head outwards (towards the liquid medium) while hiding their nonpolar tail within the binding pocket.

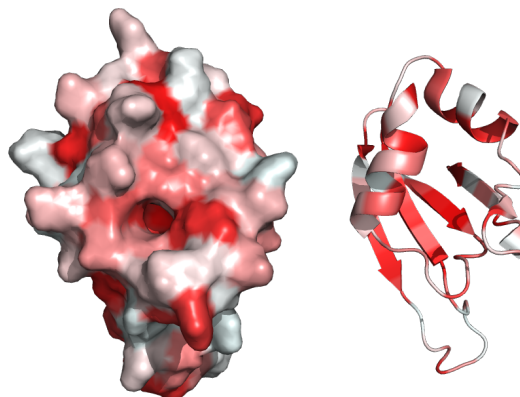


Figure 18: MSI1's RRM1 colored by aminoacid polarity. The leftmost representation is surface representation while the rightmost is the cartoon of the secondary structure. The intensity of red indicates the degree of non-polarity.

With this criterion in mind, it is easy to select the models that are less likely to happen in nature: the models in which the carboxylic group is hidden within the binding pocket.

The best structures (chosen by score and following the previous criterion) are shown in **Figure 19**:

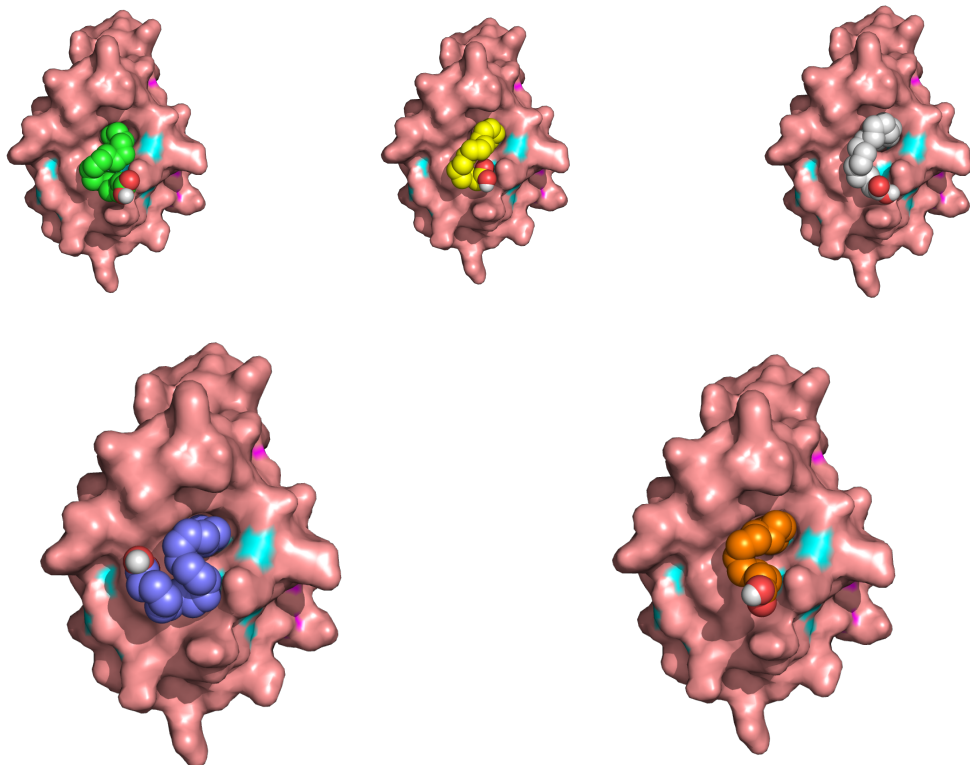


Figure 19: Top models for RRM1-fatty acid docking simulations. From left to right and top to bottom: models for RRM1-oleic acid (green), RRM1-linoleic acid (yellow), RRM1-stearic acid (white), RRM1-arachidonic acid (purple) and RRM1-palmitic acid (orange). Visualized through [Pymol](#).

The models selected are satisfactory as they hide most of the hydrophobic chain within the pocket. In addition, the polar carboxylic group interacts with the surface of the protein as expected. Apparently, the less flexible the fatty acid's chain (see for example arachidonic acid), the more constrained the interaction is and the harder it is for it actually to happen.

In contrast, short and flexible fatty acids (see for example oleic acid), the easier the interaction is and thus, it is easier for it to happen. These results agree with Clingman and colleagues' findings [16].

4.5 Lipid-protein-RNA complex visualization

The construction and visualization of the lipid-protein-RNA complexes was done by loading the protein-RNA docking models and the protein lipid docking models, and then manually superposing them so that all structures had cohesion within [Pymol](#).

Since the protein-mutant RNA motifs docking models did not reach consensus, it only is reliable to build the lipid-protein-RNA complex with the original RNA. The oleic acid-RRM1-original RNA motif complex is shown in **Figure 20**:

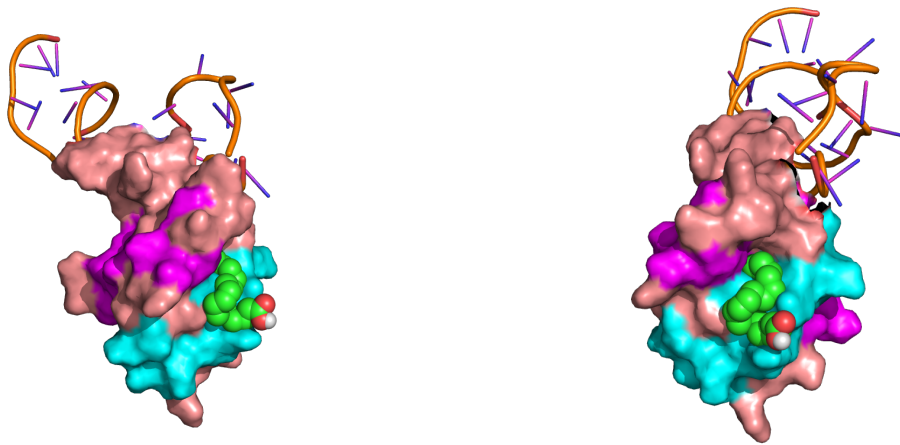


Figure 20: Oleic acid-RRM1-original RNA motif complex. The leftmost structure is a side view while the rightmost structure is a front view. Visualized through [Pymol](#).

As expected, the locations at which the RNA motif and the oleic acid attach are clearly different: the RNA motif attaches around the DPLTKRS loop while the oleic acid enters a pocket located on the opposite face of the protein. The distance among these binding sites and the size of the molecules discards the RNA-binding inhibition due to steric impediment and confirms that inhibition is in fact an allosteric behavior.

This allosterism must stem from a conformational change deep within the protein due to the non-polar nature of the oleic acid-RRM1 interaction. The conformational change must then be transmitted to the opposite face of the protein, altering the RNA binding site and thus causing a chance for release.

The remaining complexes, which originate from employing the other fatty acids, are constructed as well. These are shown in **Figure 21**:

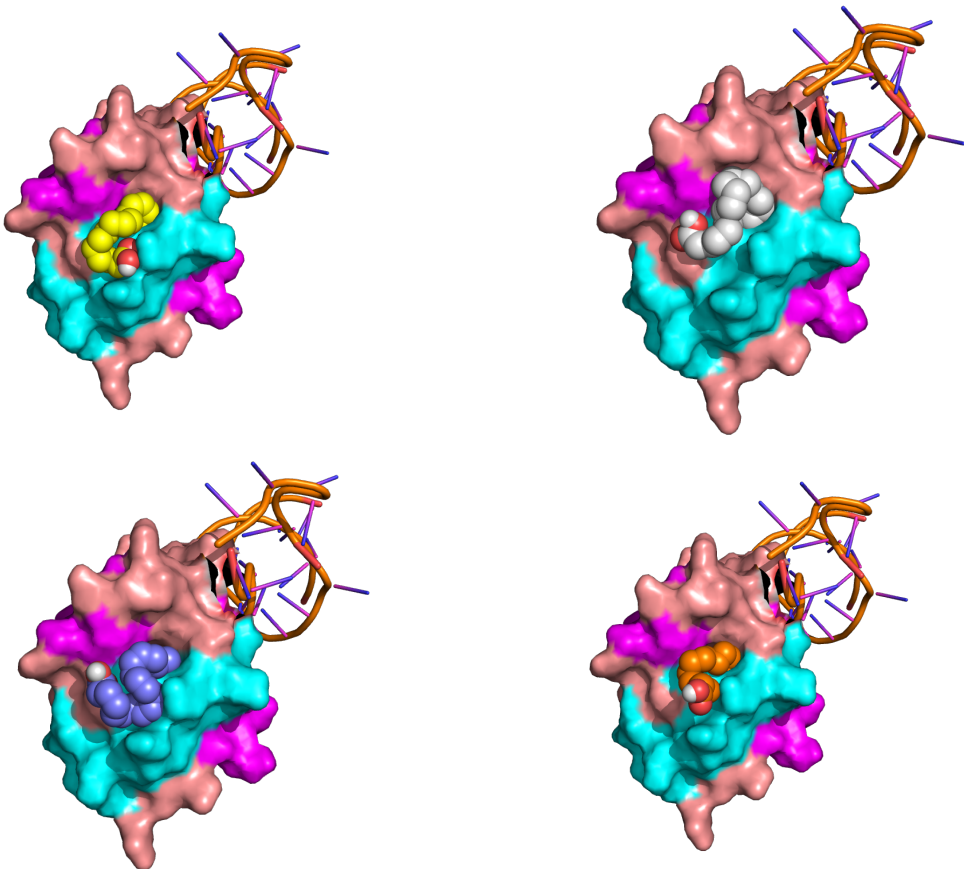


Figure 21: Top models for RRM1-fatty acid complexes. From left to right and top to bottom: models for RRM1-oleic acid (green), RRM1-linoleic acid (yellow), RRM1-stearic acid (white), RRM1-arachidonic acid (purple) and RRM1-palmitic acid (orange). Visualized through [Pymol](#).

For the remaining fatty acids, the same reasoning holds: interactions occur in different faces of the protein, and the distance among sites, plus the small size of the ligands, discard steric impediments.

5 Conclusions and further work

The main objective of this Master’s Thesis was to extend the knowledge behind of the allosteric interactions occurring in the MSI-1 proteins.

From the results observed, it can be concluded that the allosteric behavior of MSI-1 must stem from a conformational change deep within the protein, triggered by the non-polar nature of the fatty acid’s hydrocarbon chain, consequently altering the RNA binding region. The efficiency at which a particular fatty acid induces said conformational change is yet to be studied.

However, the lipid-RRM1 models hint that the smaller and more flexible the fatty acid molecule is, the more capability it may have to induce conformational changes as it can explore RRM1’s fatty acid binding “pocket” in more depth. As a consequence, the fatty acid interacts with a larger amount of aminoacids, changing their chemical environment and forcing a rearrangement that can spread to the RNA binding site.

The results obtained were partially expected: allosteric proteins undergo conformational changes when bound to their different ligands. However, it was also expected to obtain successful models for each of the RNA motif mutants to understand the effect of the RNA nucleic acid sequence itself on the interaction. Unfortunately, due to the unsatisfactory models obtained, this question will remain unanswered in this work.

The objectives stated during the initial phases of this work differ vastly from the objectives stated and accomplished in this report. Originally, each docking simulation would have been chaperoned by molecular dynamics simulations, which would have shed additional light on the matter of the allosteric behavior of RRM1. These molecular dynamics simulations were eventually scraped out from the objectives due to lack of time caused by solving troubles in the protein-RNA docking step.

Nonetheless, solving those problems resulted in a collaboration with the LightDock team for a public tutorial on how to use LightDock for protein-RNA docking, so it was worth the time.

Therefore, additional further work could be focused on molecular dynamics assays of the allosteric interactions in MSI-1, as there is expected to observe interesting conformational changes when the ligands approach and bind RRM1.

It would also be of interest to assess the strength of the protein-RNA interaction in such a way that it made possible the intelligent design of RNA ligands with pre-computed affinity.

Additionally, it would be of great benefit for the general public to extend LightDock's functionalities into lipid-protein docking, or even general small molecule-protein docking.

In sum, docking simulations have a great potential of untangling molecular mysteries such as the one involving MSI-1's allosteric nature. Nonetheless, there are still some limitations as the resulting models are not always reliable. So, there is much work to do to improve the exciting field of structural bioinformatics. Again, as Richard Feynman once said: "*what I cannot create, I do not understand*".

6 Glossary

MSI-1: Neural Musashi-1 protein.

RBP: RNA-binding protein.

RRM: RNA recognition motif

NMR: Nuclear magnetic resonance.

E. coli: *Escherichia coli*.

iGEM: International genetically engineered machine competition.

RNA: Ribonucleic acid.

RNA: Deoxyribonucleic acid.

LUCA: Last universal common ancestor.

.pdb: Protein data bank file extension.

.mol: MDL Molfile format file extension.

.fasta: FASTA format file extension.

MAFFT: Multiple alignment using fast Fourier transform algorithm.

7 References

- [1] R. Dolcemascolo, M. Heras-Hernández, L. Goiriz, R. Montagud-Martínez, A. Requena-Menéndez, R. Márquez-Costa, R. Ruiz, A. Pérez-Ràfols, R. A. Higuera-Rodríguez, G. Pérez-Ropero, W. F. Vranken, T. Martelli, W. Kaiser, J. Buijs, and G. Rodrigo, “Repurposing the mammalian rna-binding protein musashi-1 as an allosteric translation repressor in bacteria,” *bioRxiv*, 2022.
- [2] M. Nakamura, H. Okano, J. A. Blendy, and C. Montell, “Musashi, a neural rna-binding protein required for drosophila adult external sensory organ development,” *Neuron*, vol. 13, no. 1, pp. 67–81, 1994.
- [3] S. Sakakibara, T. Imai, K. Hamaguchi, M. Okabe, J. Aruga, K. Nakajima, D. Yasutomi, T. Nagata, Y. Kurihara, S. Uesugi, T. Miyata, M. Ogawa, K. Mikoshiba, and H. Okano, “Mouse-musashi-1, a neural rna-binding protein highly enriched in the mammalian cns stem cell,” *Developmental Biology*, vol. 176, no. 2, pp. 230–242, 1996.
- [4] P. Good, A. Yoda, S.-i. Sakakibara, A. Yamamoto, T. Imai, H. Sawa, T. Ikeuchi, S. Tsuji, H. Satoh, and H. Okano, “The humanmusashi homolog 1(msi1) gene encoding the homologue of musashi/nrp-1, a neural rna-binding protein putatively expressed in cns stem cells and neural progenitor cells,” *Genomics*, vol. 52, no. 3, pp. 382–384, 1998.
- [5] T. Imai, A. Tokunaga, T. Yoshida, M. Hashimoto, K. Mikoshiba, G. Weinmaster, M. Nakafuku, and H. Okano, “The neural rna-binding protein musashi1 translationally regulates mammalian numb gene expression by interacting with its mrna,” *Molecular and Cellular Biology*, vol. 21, no. 12, pp. 3888–3900, 2001.
- [6] A. Cornish-Bowden, “Nomenclature for incompletely specified bases in nucleic acid sequences: Rcommendations 1984,” *Nucleic Acids Research*, vol. 13, no. 9, pp. 3021–3030, 1985.
- [7] N. R. Zearfoss, L. M. Deveau, C. C. Clingman, E. Schmidt, E. S. Johnson, F. Massi, and S. P. Ryder, “A conserved three-nucleotide core motif defines musashi rna binding specificity,” *Journal of Biological Chemistry*, vol. 289, no. 51, pp. 35530–35541, 2014.
- [8] T. Nagata, R. Kanno, Y. Kurihara, S. Uesugi, T. Imai, S.-i. Sakakibara, H. Okano, and M. Katahira, “Structure, backbone dynamics and interactions with rna of the c-terminal rna-binding domain of a mouse neural rna-binding protein, musashi1,” *Journal of Molecular Biology*, vol. 287, no. 2, pp. 315–330, 1999.

- [9] Y. Miyanoiri, H. Kobayashi, T. Imai, M. Watanabe, T. Nagata, S. Uesugi, H. Okano, and M. Katahira, “Origin of higher affinity to rna of the n-terminal rna-binding domain than that of the c-terminal one of a mouse neural protein, musashi1, as revealed by comparison of their structures, modes of interaction, surface electrostatic potentials, and backbone dynamics,” *Journal of Biological Chemistry*, vol. 278, no. 42, pp. 41309–41315, 2003.
- [10] T. Ohyama, T. Nagata, K. Tsuda, N. Kobayashi, T. Imai, H. Okano, T. Yamazaki, and M. Katahira, “Structure of musashi1 in a complex with target rna: The role of aromatic stacking interactions,” *Nucleic Acids Research*, vol. 40, no. 7, pp. 3218–3231, 2011.
- [11] L. Lan, M. Xing, M. Kashipathy, J. Douglas, P. Gao, K. Battaile, R. Hanzlik, S. Lovell, and L. Xu, “Crystal and solution structures of human oncoprotein musashi-2 n-terminal rna recognition motif 1,” *Proteins: Structure, Function, and Bioinformatics*, vol. 88, no. 4, pp. 573–583, 2019.
- [12] J. Jumper, R. Evans, A. Pritzel, T. Green, M. Figurnov, O. Ronneberger, K. Tunyasuvunakool, R. Bates, A. Žídek, A. Potapenko, and et al., “Highly accurate protein structure prediction with alphafold,” *Nature*, vol. 596, no. 7873, pp. 583–589, 2021.
- [13] B. J. Belmont and J. C. Niles, “Engineering a direct and inducible protein-rna interaction to regulate rna biology,” *ACS Chemical Biology*, vol. 5, no. 9, pp. 851–861, 2010.
- [14] J. Cao, M. Arha, C. Sudrik, A. Mukherjee, X. Wu, and R. S. Kane, “A universal strategy for regulating mrna translation in prokaryotic and eukaryotic cells,” *Nucleic Acids Research*, vol. 43, no. 8, pp. 4353–4362, 2015.
- [15] N. Katz, R. Cohen, O. Solomon, B. Kaufmann, O. Atar, Z. Yakhini, S. Goldberg, and R. Amit, “Synthetic 5’ utrs can either up- or downregulate expression upon rna-binding protein binding,” *Cell Systems*, vol. 9, no. 1, pp. 93–106.e8, 2019.
- [16] C. C. Clingman, L. M. Deveau, S. A. Hay, R. M. Genga, S. M. Shandilya, F. Massi, and S. P. Ryder, “Allosteric inhibition of a stem cell rna-binding protein by an intermediary metabolite,” *eLife*, vol. 3, p. e02848, 2014.
- [17] R. Pereira, M. Couto, F. Ribeiro, R. Rua, J. Cunha, J. P. Fernandes, and J. Saraiva, “Energy efficiency across programming languages: How do energy, time, and memory relate?,” *Proceedings of the 10th ACM SIGPLAN International Conference on Software Language Engineering*, 2017.

- [18] T. S. Gardner, C. R. Cantor, and J. J. Collins, “Construction of a genetic toggle switch in escherichia coli,” *Nature*, vol. 403, no. 6767, pp. 339–342, 2000.
- [19] M. B. Elowitz and S. Leibler, “A synthetic oscillatory network of transcriptional regulators,” *Nature*, vol. 403, no. 6767, pp. 335–338, 2000.
- [20] The iGEM Foundation, “igem registry of standard biological parts.” http://parts.igem.org/Main_Page, 2022.
- [21] V. Siciliano, I. Garzilli, C. Fracassi, S. Criscuolo, S. Ventre, and D. di Bernardo, “Mirnas confer phenotypic robustness to gene networks by suppressing biological noise,” *Nature Communications*, vol. 4, no. 1, p. 2364, 2013.
- [22] H. Seok, H. Lee, E.-S. Jang, and S. W. Chi, “Evaluation and control of mirna-like off-target repression for rna interference,” *Cellular and Molecular Life Sciences*, vol. 75, no. 5, pp. 797–814, 2017.
- [23] P. Babitzke, C. S. Baker, and T. Romeo, “Regulation of translation initiation by rna binding proteins,” *Annual Review of Microbiology*, vol. 63, no. 1, pp. 27–44, 2009.
- [24] J. Lykke-Andersen, “Rna-protein interactions of an archaeal homotetrameric splicing endoribonuclease with an exceptional evolutionary history,” *The EMBO Journal*, vol. 16, no. 20, pp. 6290–6300, 1997.
- [25] D. E. Draper and L. P. Reynaldo, “Rna binding strategies of ribosomal proteins,” *Nucleic Acids Research*, vol. 27, no. 2, pp. 381–388, 1999.
- [26] E. Holmqvist and J. Vogel, “Rna-binding proteins in bacteria,” *Nature Reviews Microbiology*, vol. 16, no. 10, pp. 601–615, 2018.
- [27] E. V. Koonin, M. Krupovic, S. Ishino, and Y. Ishino, “The replication machinery of luca: Common origin of dna replication and transcription,” *BMC Biology*, vol. 18, no. 1, p. 61, 2020.
- [28] A. Re, T. Joshi, E. Kulberkyte, Q. Morris, and C. T. Workman, “Rna–protein interactions: An overview,” *Methods in Molecular Biology*, pp. 491–521, 2013.
- [29] M. Corley, M. C. Burns, and G. W. Yeo, “How rna-binding proteins interact with rna: Molecules and mechanisms,” *Molecular Cell*, vol. 78, no. 1, pp. 9–29, 2020.

- [30] R. Stefl, L. Skrisovska, and F. H.-T. Allain, “Rna sequence- and shape-dependent recognition by proteins in the ribonucleoprotein particle,” *EMBO reports*, vol. 6, no. 1, pp. 33–38, 2005.
- [31] J. SantaLucia, “A unified view of polymer, dumbbell, and oligonucleotide dna nearest-neighbor thermodynamics,” *Proceedings of the National Academy of Sciences*, vol. 95, no. 4, pp. 1460–1465, 1998.
- [32] R. M. Dirks and N. A. Pierce, “An algorithm for computing nucleic acid base-pairing probabilities including pseudoknots,” *Journal of Computational Chemistry*, vol. 25, no. 10, pp. 1295–1304, 2004.
- [33] Theoretical Biochemistry Group, Universität Wien, “Representations of rna secondary structures.” https://www.tbi.univie.ac.at/RNA/ViennaRNA/doc/html/rna_structure_notations.html, 2020.
- [34] K. Katoh, K. Misawa, K. Kuma, and T. Miyata, “Mafft: A novel method for rapid multiple sequence alignment based on fast fourier transform,” *Nucleic Acids Research*, vol. 30, no. 14, pp. 3059–3066, 2002.
- [35] M. Biesiada, K. Purzycka, M. Szachniuk, J. Blazewicz, and R. Adamiak, “Automated rna 3d structure prediction with rnacomposer,” *RNA Structure Determination: Methods and Protocols*, pp. 199–215, 2016.
- [36] B. Jiménez-García, J. Roel-Touris, M. Romero-Durana, M. Vidal, D. Jiménez-González, and J. Fernández-Recio, “Lightdock: A new multi-scale approach to protein-protein docking,” *Bioinformatics*, vol. 34, no. 1, pp. 49–55, 2017.
- [37] J. Rodrigues, J. Teixeira, M. Trellet, and A. Bonvin, “pdb-tools: a swiss army knife for molecular structures,” *F1000Research*, vol. 7, no. 1961, 2018.
- [38] Amber biomolecular simulation package, “Amber histidine residues.” <http://ambermd.org/Questions/HIS.html>, 2005.

8 Appendix

Appendix A: RNA motifs employed in this work, as seen in [1] (in .fasta format)

```
1 >orig
2 GGCAGCGUUAGUUUUAGUUCGUAUGCC
3 >mut1
4 GGCAGCGUUUCGUUAAAAGUUCGUAUGCC
5 >mut2
6 GGCAGCGUUACUUAAAAGUUCGUAUGCC
7 >mut3
8 GGCAGCGUUAGCUAAAAGUUCGUAUGCC
9 >mut4
10 GGCAGCGUUAGUUAUGUUAGUUCGUAUGCC
11 >mut5
12 GGCAGCGUUACUUAAAACUUCGUAUGCC
```

Appendix B: Python script to treat the RNA motifs

```
1 import os
2 import datetime
3 import Bio.SeqIO
4 import pandas as pd
5 import nupack as npk
6 from hashlib import sha256
7 from subprocess import Popen, PIPE
8
9 # Global vars
10 modelRNA = npk.Model(
11     material="rna95-nupack3",
12     ensemble="some-nupack3",
13     celsius=37,
14     sodium=1.0,
15     magnesium=0.0
16 )
17
18 # Functions
19
20 def alignment(reference:str, case:str) -> str:
21
22     # Absolutely unique name
23     name = (
24         sha256(bytes(str(datetime.datetime.now()), "UTF-8")).hexdigest()
25         + ".fasta"
26     )
```

```
27     with open(name, "w") as file:
28         file.write(
29             f">reference\n{reference}\n>case\n{case}\n"
30         )
31
32     process = Popen(
33         ["mafft", "--clustalout", name],
34         stdout=PIPE, stderr=PIPE
35     )
36
37
38     # Should never fail, so I won't check the stderr
39     stdout = process.communicate()[0]
40
41     os.remove(name)
42
43     alignInfo = stdout.decode("UTF-8").split("\n")
44
45     return alignInfo[5][-max(len(reference), len(case)):]
46
47 def folding(seq:str) -> str:
48
49     mfe_structures = npk.mfe(
50         strands=[seq],
51         model=modelRNA
52     )
53
54     return str(mfe_structures[0].structure)
55
56 def get_data_RNAcomposer(df:pd.DataFrame) -> None:
57
58     series = df.apply(
59         lambda row:
60             "\n".join([
61                 ">" + row["name"],
62                 row["seq"],
63                 row["structure"]
64             ]),
65             axis=1
66     )
67
68     for el in series:
69         print(el)
70
71     return None
72
73
74 def main():
75
```

```
76     # Read sequences into data frame
77     seqs = pd.DataFrame([
78         (record.id, str(record.seq))
79         for record in
80         Bio.SeqIO.parse("../data/motifs.fasta", "fasta")
81     ])
82
83     seqs.columns = ("name", "seq")
84
85     seqs["alignment"] = seqs["seq"].apply(
86         lambda seq: alignment(seqs.loc[0, "seq"], seq)
87     )
88
89     seqs["structure"] = seqs["seq"].apply(
90         lambda seq: folding(seq)
91     )
92
93     return seqs
94
95
96
97 if __name__ == "__main__":
98     s = main()
99     print(s)
```

Appendix C: Python script to relabel HIS residues for their corresponding AMBER94 compatible residues

```
1 import sys
2 from lightdock.scoring.dna.data.amber import atoms_per_residue
3
4 """http://ambermd.org/Questions/HIS.html
5
6 AMBER Histidine residues
7
8 Histidine (HIS in normal pdb files) is really one of three
9     possible residues:
10 HID: Histidine with hydrogen on the delta nitrogen
11 HIE: Histidine with hydrogen on the epsilon nitrogen
12
13 HIP: Histidine with hydrogens on both nitrogens; this is
14     positively charged.
15 It is up to the user to inspect the environment of each histidine
16     and identify the type that is appropriate.
17 """
```

```
18
19 hists = {
20     k:sorted([atom for atom in v if atom.startswith("H")])
21     for k,v in atoms_per_residue.items()
22     if k.startswith("HI"))
23 }
24
25 content = ""
26
27 with open(sys.argv[1]) as file:
28
29     isHis = False
30     HisH = []
31     histinfo = ""
32
33     for line in file:
34         elems = line.split()
35
36         if elems[0] == "ATOM":
37
38             if elems[3] == "HIS":
39
40                 isHis = True
41                 histinfo += line
42
43                 if elems[-2] == "H":
44                     HisH.append(elems[2])
45
46                 continue
47
48             elif isHis:
49                 isHis = False
50                 key = [k for k,v in hists.items() if v == sorted(
HisH)][0]
51
52                 content += (
53                     histinfo.replace("HIS", key)
54                     + line
55                 )
56
57                 HisH = []
58                 histinfo = ""
59                 continue
60
61             else:
62                 content += line
63                 continue
64
65             content += line
```

```
66
67 print(content)
```

Appendix D: Python script to remove 3' and 5' hydroxile groups in the RNA structures

```
1 import sys
2
3 with open(sys.argv[1]) as file:
4     filelines = filter(
5         lambda line:
6             (line.find("H05") < 0)
7             and (line.find("H03") < 0)
8         ),
9         file.readlines()
10    )
11
12 print("".join(filelines))
```

Appendix E: Python script to rename and remove incompatible atom types from the RNA srtructure

```
1 #!/usr/bin/env python3
2
3 # NOTE BY LUCAS (NOVEMBER 2022):
4 # use this on .pdb files corresponding to RNA structures only!
5
6 """
7 ATOM      23  H5'   DG B   1    -15.347   -3.940   -5.934   1.00   0.00
8          H      new
9 ATOM      24  H5'   DG B   1    -15.852   -4.851   -7.094   1.00   0.00
10         H     new
11 ATOM      25  H4'   DG B   1    -15.214   -3.222   -8.238   1.00   0.00
12         H     new
13 ATOM      26  H3'   DG B   1    -13.483   -5.075   -8.732   1.00   0.00
14         H     new
15 ATOM      27  H2'   DG B   1    -11.785   -4.224   -7.287   1.00   0.00
16         H     new
17 ATOM      28  H2'   DG B   1    -11.314   -3.732   -8.690   1.00   0.00
18         H     new
19 ATOM      29  H1'   DG B   1    -12.430   -1.717   -8.491   1.00   0.00
20         H     new
21 ATOM      30  H8    DG B   1    -10.897   -3.080   -5.447   1.00   0.00
22         H     new
23 ATOM      31  H1    DG B   1    -10.070    2.951   -6.160   1.00   0.00
24         H     new
25 ATOM      32  H21   DG B   1    -12.087   2.806   -8.716   1.00   0.00
26         H     new
```

```
17 ATOM      33   H22    DG B    1      -11.235     3.696   -7.879   1.00   0.00
18      H    new
19
20 import os
21 import argparse
22 from lightdock.scoring.dna.data.amber import atoms_per_residue
23 from lightdock.pdbutil.PDBIO import read_atom_line
24
25
26 def _format_atom_name(atom_name):
27     """Format ATOM name with correct padding"""
28     if len(atom_name) == 4:
29         return atom_name
30     else:
31         return "%s" % atom_name
32
33
34 def write_atom_line(atom, output):
35     """Writes a PDB file format line to output."""
36     if atom.__class__.__name__ == "HetAtom":
37         atom_type = "HETATOM"
38     else:
39         atom_type = "ATOM"
40     line = "%6s%5d %-4s%-1s%3s%2s%4d%1s    %8.3f%8.3f%8.3f%6.2f%6.2f%12s\n" %
41           atom_type,
42           atom.number,
43           _format_atom_name(atom.name),
44           atom.alternative,
45           atom.residue_name,
46           atom.chain_id,
47           atom.residue_number,
48           atom.residue_insertion,
49           atom.x,
50           atom.y,
51           atom.z,
52           atom.occupancy,
53           atom.b_factor,
54           atom.element,
55       )
56     output.write(line)
57
58
59 translation = {
60     "H5'": "H5'1",
61     "H5'': "H5'2",
62     "H2'": "H2'1",
63     "H2'': "H2'2",
```

```
64     "H02'": "HO'2", # These ones were added by Lucas in November
65     "H03'": "HO'3", #
66     "H05'": "HO'5"  #
67 }
68
69
70 if __name__ == "__main__":
71
72     parser = argparse.ArgumentParser()
73     parser.add_argument("input_pdb_file")
74     parser.add_argument("output_pdb_file")
75     args = parser.parse_args()
76
77     with open(args.input_pdb_file) as ih:
78         with open(args.output_pdb_file, 'w') as oh:
79             for line in ih:
80                 line = line.rstrip(os.linesep)
81                 if line.startswith("ATOM "):
82                     atom = read_atom_line(line)
83
84                     # The following lines were added by Lucas in
85                     # November 2022 #
86                     if (
87                         # not(atom.residue_name.startswith("R"))
88                         # and not(atom.residue_name.startswith("D"))
89                         # ):
90                         # atom.residue_name = "R" + atom.
91                         residue_name
92                         #
93                         #####
94                         if atom.residue_name not in atoms_per_residue:
95                             print(f"Not supported atom: {atom.
96                         residue_name}.{atom.name}")
97                         else:
98                             if atom.name not in atoms_per_residue[atom
99                             .residue_name] and atom.is_hydrogen():
100                                try:
101                                    atom.name = translation[atom.name]
102                                    write_atom_line(atom, oh)
103                                except KeyError:
104                                    print(f"Atom not found in mapping:
105 {atom.residue_name}.{atom.name}")
106                                else:
107                                    write_atom_line(atom, oh)
```

Appendix F: Python script to remove the incompatible R tags from the RNA structures

```
1 import sys
2
3 def reemplazar(line):
4     line = list(line)
5     line[line.index("R")] = " "
6     return "".join(line)
7
8 with open(sys.argv[1]) as file:
9     lines = file.readlines()
10
11
12 S = list(map(
13     reemplazar,
14     lines
15 ))
16
17 with open(sys.argv[1], "w") as file:
18     file.write("".join(S))
```

Appendix G: Python script to recover the R tags from the RNA structures

```
1 import sys
2
3 with open(sys.argv[1]) as file:
4
5     filelines = file.readlines()
6
7
8 nufilelines = list(map(
9     lambda line: (
10         line
11         .replace(" A A", " RA A")
12         .replace(" U A", " RU A")
13         .replace(" G A", " RG A")
14         .replace(" C A", " RC A")
15         .replace(" A B", " RA B")
16         .replace(" U B", " RU B")
17         .replace(" G B", " RG B")
18         .replace(" C B", " RC B")
19     ),
20     filelines
21 ))
22
23 with open(sys.argv[1], "w") as file:
```

```
24     file.write("".join(nufilelines))
```

Appendix H: Bash script to cluster and rank the models generated by LightDock

```
1 ## Calculate the number of swarms
2 s='ls -d ./swarm_* | wc -l'
3 swarms=$((s-1))

4
5 ## Create files for Ant-Thony
6 for i in $(seq 0 $swarms)
7   do
8     echo "cd swarm_${i}; lgd_generate_conformations.py ../protein.
      pdb ../rna.pdb gso_100.out 200 > /dev/null 2> /dev/null;" >>
      generate_lightdock.list;
9   done

10
11 for i in $(seq 0 $swarms)
12   do
13     echo "cd swarm_${i}; lgd_cluster_bsas.py gso_100.out > /dev/
      null 2> /dev/null;" >> cluster_lightdock.list;
14   done

15
16 ### Generate LightDock models
17 ant_thony.py -c 4 generate_lightdock.list;
18
19 ### Clustering BSAS (rmsd) within swarm
20 ant_thony.py -c 4 cluster_lightdock.list;
21
22 ### Generate ranking files for filtering
23 lgd_rank.py $s 100;
```

Appendix I: Bash script to run a complete protein-RNA docking simulation with LightDock

```
1 # Parse inputs
2 proteinPDBpath=$1
3 ligandPDBpath=$2
4
5 IFS='/' read -r -a tmp <<< "$proteinPDBpath"
6 IFS='.' read -r -a proteinPDBfilename <<< "${tmp[$#tmp[@]}-1]}"
7
8 IFS='/' read -r -a tmp <<< "$ligandPDBpath"
9 IFS='.' read -r -a ligandPDBfilename <<< "${tmp[$#tmp[@]}-1]}"
10
11 echo ">>>Inputs used are: $proteinPDBfilename and
      $ligandPDBfilename"
12
```

```
13 # Protonation
14 ## Case 1: protein.
15
16 echo ">>>CASE 1: protein."
17 echo ">>>Remove the previous hydrogens and them rebuild them
18 according to reduce"
19
20 reduce -Trim $proteinPDBpath > "${proteinPDBfilename}_noh.pdb"
21 reduce -BUILD "${proteinPDBfilename}_noh.pdb" > "${proteinPDBfilename}_h.pdb"
22
23 echo ">>>Renumber the atoms of the protein receptor partner using
24 PDB-Tools"
25
26 pdb_reatom "${proteinPDBfilename}_h.pdb" > protein_pre.pdb
27
28 echo ">>>Fix HIS residues so that they work with AMBER force field
29 "
30
31 python3.9 ../../../../fixHIS.py protein_pre.pdb > protein.pdb
32
33 ## Case 2: RNA motif.
34
35 echo ">>>CASE 2: RNA ligand."
36 echo ">>>Remove the previous hydrogens and them rebuild them
37 according to reduce"
38
39 reduce -Trim $ligandPDBpath > "${ligandPDBfilename}_noh.pdb"
40 reduce -BUILD "${ligandPDBfilename}_noh.pdb" > "${ligandPDBfilename}_h.pdb"
41
42 echo ">>>Remove possible top overhang OH"
43
44 python3.9 ../../../../removeEnds.py "${ligandPDBfilename}_h.pdb" > "${ligandPDBfilename}_nvh.pdb"
45
46 echo ">>>Rename and/or remove incompatible atom types of RNA"
47
48 python3.9 ../../../../reduce_to_amber.py "${ligandPDBfilename}_nvh.
49     pdb" rna.pdb
50
51 python3.9 ../../../../manipulateRNA.py rna.pdb
52
53 # Setup
54
55 echo ">>>Make lightdock setup"
56
57 # Without restraints
58 lightdock3_setup.py protein.pdb rna.pdb -anm
```

```
54
55
56 # Simulation
57 echo ">>>Recover RNA tags in lightdock_rna.pdb"
58
59 python3.9 ../../../../manipulateRNAagain.py lightdock_rna.pdb
60
61 echo ">>>Make lightdock simulation"
62
63 lightdock3.py setup.json 100 -s dna -c 4
64
65 # Clustering
66 echo ">>>Do clustering and filtering"
67
68 python3.9 ../../../../manipulateRNA.py lightdock_rna.pdb
69
70 ## Calculate the number of swarms
71 s='ls -d ./swarm_* | wc -l'
72 swarms=$((s-1))
73
74 ## Create files for Ant-Thony
75 for i in $(seq 0 $swarms)
76   do
77     echo "cd swarm_${i}; lgd_generate_conformations.py ../protein.
    pdb ../rna.pdb gso_100.out 200 > /dev/null 2> /dev/null;" >>
      generate_lightdock.list;
78   done
79
80 for i in $(seq 0 $swarms)
81   do
82     echo "cd swarm_${i}; lgd_cluster_bsas.py gso_100.out > /dev/
      null 2> /dev/null;" >> cluster_lightdock.list;
83   done
84
85 ### Generate LightDock models
86 ant_thony.py -c 4 generate_lightdock.list;
87
88 ### Clustering BSAS (rmsd) within swarm
89 ant_thony.py -c 4 cluster_lightdock.list;
90
91 ### Generate ranking files for filtering
92 lgd_rank.py $s 100;
```

Appendix J: Contents of the grid file employed during the protein-lipid docking simulations

```
1 protein
2 spacing      0.331
3 npts        22 22 20
4 center       0.732 -3.346 -9.863
```

Appendix K: Contents of the config file employed during the protein-lipid docking simulations

```
1 receptor = protein.pdbqt
2 ligand = ligand.pdbqt
3
4 center_x = 0.732
5 center_y = -3.346
6 center_z = -9.863
7
8 size_x = 22
9 size_y = 22
10 size_z = 30
11
12 energy_range = 4
13
14 exhaustiveness = 8
```